Supporting information for

Top-Contacting Molecular Monolayers using Single Crystalline Au Microplate Electrodes

*B. Radha, Deepak Jayaraj and G. U. Kulkarni**

Methods and Materials:

Synthesis of Au microplate electrodes

Au microplate synthesis in detail is reported elsewhere.[1,2] Briefly, the precursor complex for microplate synthesis i.e., $(AuCl_4)^-$–tetraoctylammonium bromide complex was prepared by phase transfer of $(AuCl_4)^-$ ions from an aqueous solution (25 mmol/L, 3.2 mL) to toluene (8 mL) using ToABr (50 mmol/L) as phase transfer agent. The organic layer was separated and drop coated onto glass substrate. Thermolysis was carried out in air at 130 °C for up to 55 h. Following thermolysis, a gentle wash in toluene, followed by ethanol and water was carried out to remove any remaining precursor on the microplates. The resulting Au microplates were examined using an optical microscope (Laben, India).

Fabrication of the molecular device

The device fabrication starts with well cleaned glass slides which were deposited with a thin (~40 nm) layer of Au by PVD (HindHivac, India) at a base pressure of 10^{-6} torr. This serves as bottom electrode of the micro-sandwich. Shadow masking resulted in two electrically isolated Au pads. The synthesized Au microplates can be easily manipulated using sharp metal pins attached to 3-axis differential micrometer driven stage (Nanomax TS from Thorlabs) or manually using an improvised micromanipulating tool developed by longitudinally inserting a chemically etched

sharp Cu wire into a capillary tube. A microplate was marshaled (using either of the methods stated above) towards the gap at the end of one Au contact pad on glass. Then, a carbon fibre, coated with Pd hexadecylthiolate on both ends, and air-dried was placed with its one end over the Au microplate electrode and the other end resting over the adjacent electrically isolated Au contact pad. Then the entire system was heated on a hot plate in ambient at 250 °C for 1 hr. Pd hexadecylthiolate acts as a nanosolder[3] after thermolysis leading to a robust electrical contact between the C-fibre and the Au electrodes.

Self-assembly of molecules and characterization

The molecules were self-assembled between the top and bottom electrodes, formed by the Au microplate and the Au contact pad respectively, by immersing the device in a 50 mM solution of the desired alkanethiol or alkanedithiol in toluene overnight (Figure 1b). After the self-assembly, the device was washed carefully with excess toluene and gently dried with N_2 and then the devices were ready for further electrical and mechanical analysis. Current–voltage measurements were done using a Keithley 236 source measure unit. Temperature controlled experiments were done by placing the sample on a temperature controlled stage (Linkam scientific instruments, UK) with a precision of 0.01 °C. For recording the raman spectrum, the wavelength of excitation was 532 nm; the power at the sample was 5 mW; the signal accumulation was for 10 s with a spectral resolution of 2 cm^{-1}. For making thin layers of PVA (molecular weight 130K from Sigma aldrich), 1 wt% solution in water was used. For PDMS films, sylgard 184 curing agent (Dow Corning) and its elastomer were mixed in the ratio of 1:10 by weight. The mixture was then degassed under vacuum for 30 min. The mixture was spin coated at 2000 rpm for 60s. Thermal curing of PDMS was done at room temperature (28 °C) for 12 hrs. Mechanical analysis for the molecular junctions was performed by placing known standard weights on top of the encapsulated device. Prior to

mechanical analysis, a thicker (~30-50 μm) layer of PDMS was placed as extra cushion on the device so as to prevent any possible disturbance while adding the weights.

Figure S1. Roughness of bottom Au thin film electrode

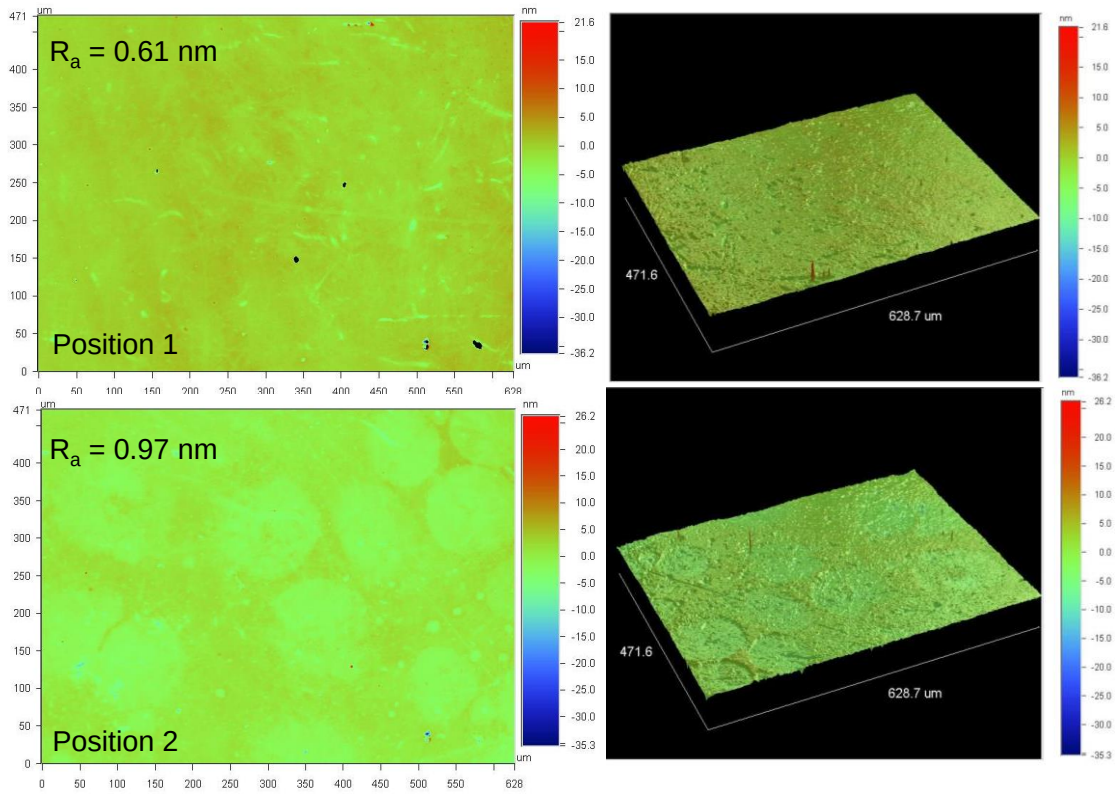

Figure S1. Optical profilometric images and 3D projected views of thin film of Au, deposited by physical vapor deposition on glass. The images are taken from two different areas of the film. Average roughness of the film is less than 1 nm.

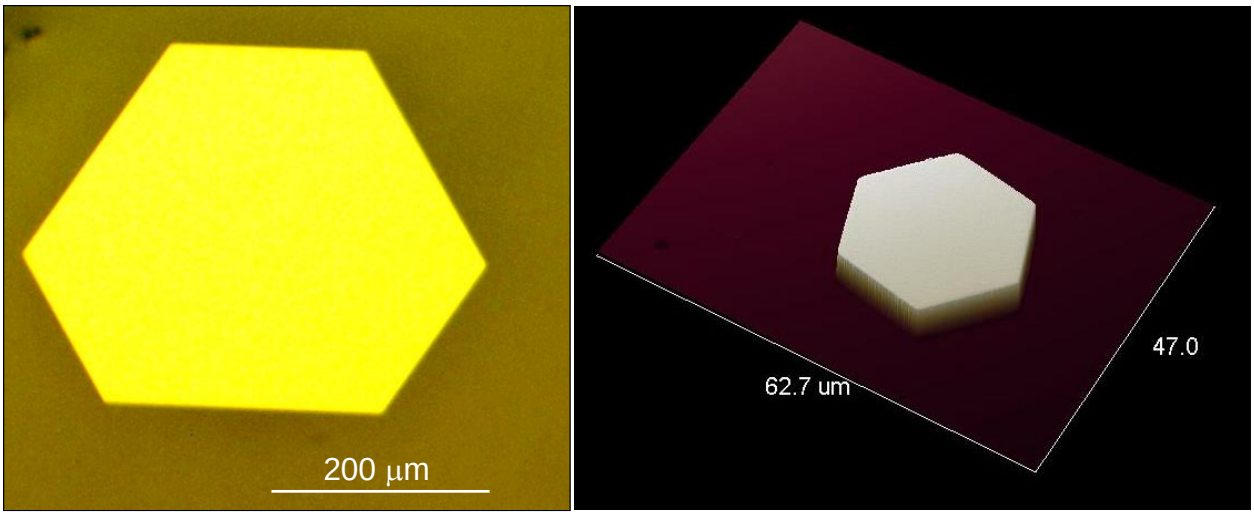

Figure S2. Optical (left) and profilometric (right) images of a Au microplate. The roughness measured from profilometric image over many areas, was ~1-2 nm.

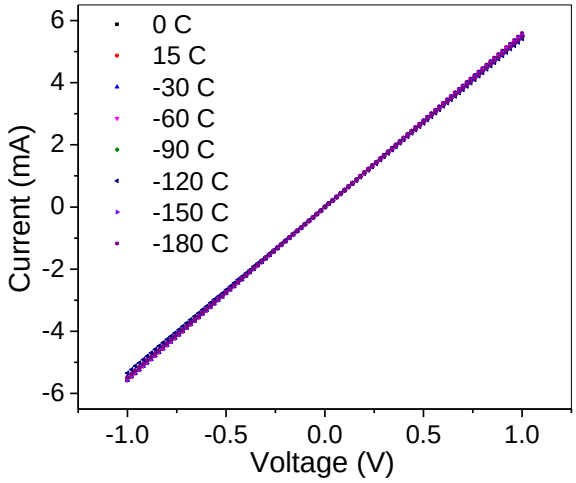

Figure S3. Temperature independent I-V characteristics of a C8D molecular device showing the typical tunneling behavior.

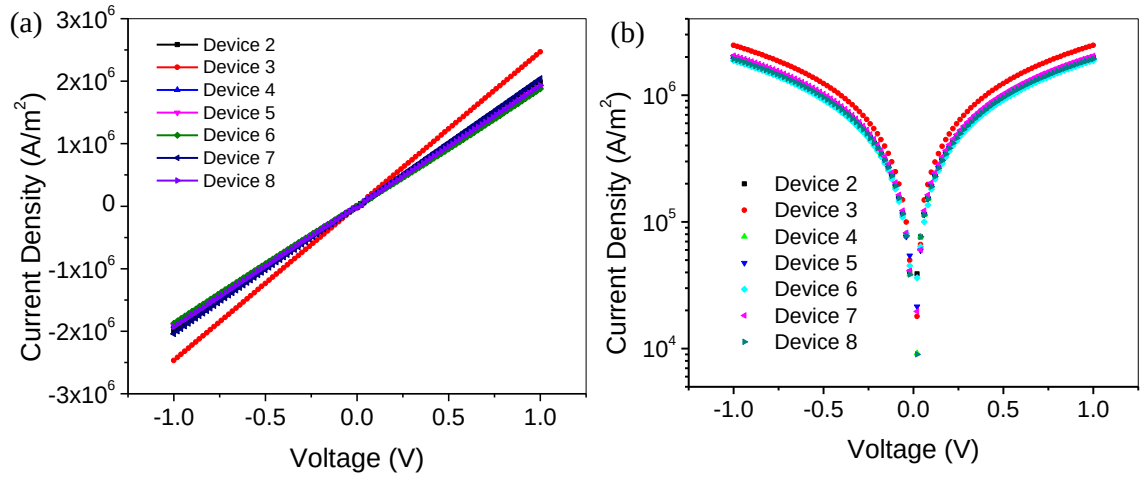

Figure S4. Device statistics: J-Vs of seven more molecular junctions of octanedithiol in (a) linear and (b) log scale.

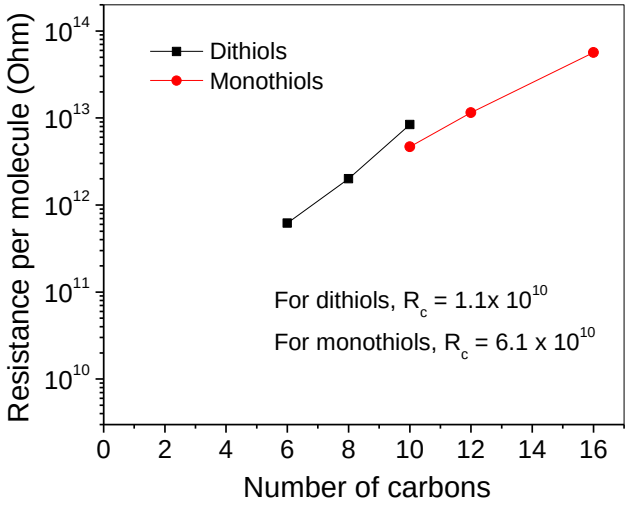

Figure S5. Resistance of single molecule, plotted versus number of carbons of the alkanethiol and dithiol molecules probed in the molecular junction device.

Table S1. Decay constant, β values typically observed in various methods of probing molecular junctions.

S. No.	Technique	Electrical contacts	Number of carbons	Beta (per carbon)	Ref
1	STM	Au-S/S-Au Au-NH_2/NH_2-Au Au-COO/COO-Au	6,8,10	1.08 0.88 0.77	4
2	STM –molecular wires	Au-S/S-Au	6,8,9	0.51	5
3	STM – Break junctions	Au-S/S-Au	6,8	0.99	6
4	STM	Au-S/S-Au	6,8,10	1.09	7
5	STM	Au-NH_2/NH_2-Au	2,3,4,5,6,7,8	0.86	8
6	C-AFM	Au-S/CH_3-Au	6,7,8,9,10	1.45	9
7	C-AFM	Au-S/S-Au Au-S/CH_3-Au	2,4,6,7,8 2,3,4,6,8,10	1.17 0.99	10
8	C-AFM	Au-S/CH_3-Au	6,8,10,12	1.01	11
9	Nanoparticle AFM	Au-S/S-Au	8,10,12	0.54	12
10	Nanoparticle AFM	Au-S/S-Au	8,10,12	1	13
11	Hanging Hg drop junction	Au-S/S-Hg	9,10,11,12,15,16,18 16,18,20,22,24	1.06 1.01	14
12	Hanging Hg drop junction	Au-S/S-Hg	20,24,28	0.85	15
13	Nanopores	Au-S/CH_3-Au	8,12,16	0.83	16
14	Large area junction	Au-S/CH_3/polymer-Hg	8,10,12,14,16	1.13	17
15	Large Area junction	Au-S/SH-PEDOT	8,10,12,14,16	0.66	18, 19
16	Nanoparticle molecular bridges	Au-S/CH_3-Au/Au-CH_3/S-Au	6,10,12	0.87	20
17	Polymer-assisted lift-off (PALO)	Al_2O_3OCO/CH_3-Au	17,18,19,20,21,22	0.85	21
18	Surface diffusion mediated deposition	Au-S/CH_3-pyrolysed photoresist film	8,10,12	1.1	22
19	Thermally evaporated	Au-S/CH_3-Au	8,12,16	1.08	23

20	Multi-layer Graphene electrode	Au-S/CH_3-Graphene-Au	8,12,16	1.06	24
21	Solution-Processed Ultrathin graphene electrode	Au-S/CH_3-Graphene-Au	8,12,16	0.7	25
22	Eutectic Gallium–Indium electrode	Ag-S/CH_3-Ga_2O_3-EGaIn	10,12,14,16 9,11,13,15,17	1.024 1.053	26
23	STM	Au-C/C-Au	4,8,10,12	0.97	27
24	Strained nanomembranes	Au-S/CH_3-Au	7,9,11,13,15	1.01	28
25	Inelastic electron tunneling spectroscopy	Au-S/S-Au	8,9,10,11,12	0.88	29
26	STM	Au-S/COO-Au	1,2,3,4	0.9	30
27	C-AFM and nanodot	Au-S/CH_3-Au	8,12,18	0.95	31

References:

(1) Radha, B.; Kulkarni, G. U. *Crystal Growth & Design* **2011**, *11*, 320.

(2) Radha, B.; Kulkarni, G. U. *Current Science* **2012**, *102*, 70.

(3) Bhuvana, T.; Smith, K. C.; Fisher, T. S.; Kulkarni, G. U. *Nanoscale* **2009**, *1*, 271.

(4) Chen, F.; Li, X.; Hihath, J.; Huang, Z.; Tao, N. *Journal of the American Chemical Society* **2006**, *128*, 15874.

(5) Haiss, W.; Nichols, R. J.; van Zalinge, H.; Higgins, S. J.; Bethell, D.; Schiffrin, D. J. *Physical Chemistry Chemical Physics* **2004**, *6*, 4330.

(6) Suzuki, M.; Fujii, S.; Fujihira, M. *Jpn. J. Appl. Phys.* **2006**, *45*, 2041.

(7) Xu, B.; Tao, N. J. *Science* **2003**, *301*, 1221.

(8) Venkataraman, L.; Klare, J. E.; Tam, I. W.; Nuckolls, C.; Hybertsen, M. S.; Steigerwald, M. L. *Nano Letters* **2006**, *6*, 458.

(9) Wold, D. J.; Frisbie, C. D. *Journal of the American Chemical Society* **2000**, *122*, 2970.

(10) Engelkes, V. B.; Beebe, J. M.; Frisbie, C. D. *Journal of the American Chemical Society* **2004**, *126*, 14287.

(11) Beebe, J. M.; Engelkes, V. B.; Miller, L. L.; Frisbie, C. D. *Journal of the American Chemical Society* **2002**, *124*, 11268.

(12) Cui, X. D.; Primak, A.; Zarate, X.; Tomfohr, J.; Sankey, O. F.; Moore, A. L.; Moore, T. A.; Gust, D.; Nagahara, L. A.; Lindsay, S. M. *The Journal of Physical Chemistry B* **2002**, *106*, 8609.

(13) Morita, T.; Lindsay, S. *Journal of the American Chemical Society* **2007**, *129*, 7262.

(14) York, R. L.; Nguyen, P. T.; Slowinski, K. *Journal of the American Chemical Society* **2003**, *125*, 5948.

(15) Weiss, E. A.; Chiechi, R. C.; Kaufman, G. K.; Kriebel, J. K.; Li, Z.; Duati, M.; Rampi, M. A.; Whitesides, G. M. *Journal of the American Chemical Society* **2007**, *129*, 4336.

(16) Wang, W. Y.; Lee, T.; Reed, M. A. *Physical Review B* **2003**, *68*.

(17) Milani, F.; Grave, C.; Ferri, V.; Samorì, P.; Rampi, M. A. *ChemPhysChem* **2007**, *8*, 515.

(18) Akkerman, H. B.; Kronemeijer, A. J.; van Hal, P. A.; de Leeuw, D. M.; Blom, P. W. M.; de Boer, B. *Small* **2008**, *4*, 100.

(19) Akkerman, H. B.; Blom, P. W. M.; de Leeuw, D. M.; de Boer, B. *Nature* **2006**, *441*, 69.

(20) Chu, C.; Na, J.-S.; Parsons, G. N. *Journal of the American Chemical Society* **2007**, *129*, 2287.

(21) Shimizu, K. T.; Fabbri, J. D.; Jelincic, J. J.; Melosh, N. A. *Advanced Materials* **2006**, *18*, 1499.

(22) Bonifas, A. P.; McCreery, R. L. *Nature Nanotechnology* **2010**, *5*, 612.

(23) Kim, T.-W.; Wang, G.; Lee, H.; Lee, T. *Nanotechnology* **2007**, *18*, 315204.

(24) Wang, G.; Kim, Y.; Choe, M.; Kim, T.-W.; Lee, T. *Advanced Materials* **2011**, *23*, 755.

(25) Li, T.; Hauptmann, J. R.; Wei, Z.; Petersen, S.; Bovet, N.; Vosch, T.; Nygård, J.; Hu, W.; Liu, Y.; Bjørnholm, T.; Nørgaard, K.; Laursen, B. W. *Advanced Materials* **2012**, *24*, 1333.

(26) Thuo, M. M.; Reus, W. F.; Nijhuis, C. A.; Barber, J. R.; Kim, C.; Schulz, M. D.; Whitesides, G. M. *Journal of the American Chemical Society* **2011**, *133*, 2962.

(27) Cheng, Z. L.; Skouta, R.; Vazquez, H.; Widawsky, J. R.; Schneebeli, S.; Chen, W.; Hybertsen, M. S.; Breslow, R.; Venkataraman, L. *Nature Nanotechnology* **2011**, *6*, 353.

(28) Bof Bufon, C. C.; Arias Espinoza, J. D.; Thurmer, D. J.; Bauer, M.; Deneke, C.; Zschieschang, U.; Klauk, H.; Schmidt, O. G. *Nano Letters* **2011**, *11*, 3727.

(29) Song, H.; Kim, Y.; Jeong, H.; Reed, M. A.; Lee, T. *The Journal of Physical Chemistry C* **2010**, *114*, 20431.

(30) Ahn, S.; Aradhya, S. V.; Klausen, R. S.; Capozzi, B.; Roy, X.; Steigerwald, M. L.; Nuckolls, C.; Venkataraman, L. *Physical Chemistry Chemical Physics* **2012**, *14*, 13841.

(31) Smaali, K.; Clément, N.; Patriarche, G.; Vuillaume, D. *ACS Nano* **2012**, *6*, 4639.

Table S2.

Device No.	Reference	Current at 0.5 V (mA)	Device Area (μm^2)	Current Density at 0.5 V (x 10^6 A/m^2)
1	Figure 2a and 2b	2.7	2344	1.150
2	Figure S4	7.5	7694	0.980
3	Figure S4	11.6	9398	1.240
4	Figure S4	7.2	7497	0.956
5	Figure S4	8.2	8610	0.955
6	Figure S4	6.4	6986	0.917
7	Figure S4	2.2	2173	1.020
8	Figure S4	9.2	9608	0.958
Average current density				1.022
Standard deviation				0.113